

Surfactant Assisted Synthesis of Rod-like LiFePO₄/C Composite with Cluster Texture as Cathode Material for Lithium Ion Batteries

Yaochun Yao^{1,2,3}, Xiaopeng Huang^{1,2,3}, Dan Zhou^{1,2,3}, Bin Yang^{1,2,3}, Wenhui Ma and Feng Liang^{1,2,3,*}

¹ Faculty of Metallurgical and Energy Engineering, Kunming University of Science and Technology, Kunming 650093, China

² Engineering Laboratory for Advanced Batteries and Materials of Yunnan Province, Kunming University of Science and Technology, Kunming 650093, China

³ National Engineering Laboratory for Vacuum Metallurgy, Kunming 650093, China

*E-mail: liangfeng@kmust.edu.cn

Received: 6 September 2018 / Accepted: 29 October 2018 / Published: 7 February 2019

Rod-like LiFePO₄/C composite with cluster texture is successfully fabricated by a solvothermal method using polyethylene glycol (PEG) and water as co-solvent. The cetyltrimethyl ammonium bromide (CTAB) has been utilized as surfactant and found to play a crucial role for tailoring active material properties (e.g., crystal orientation, particle morphology, and electrochemical performance). This can be ascribed to the dual function of CTAB: adhering onto the special crystal surface for unique morphology, and acting as templet for the self-assembly. A reasonable growth mechanism of LiFePO₄/C particles with or without CTAB is proposed. By introducing 3 mmol CTAB surfactant, rod-like LiFePO₄/C composite with cluster texture is obtained, which exhibits good rate performance of 152.3 mAh/g at 0.2C and 90.9 mAh/g at 10C.

Keywords: Lithium ion batteries, Rod-like, LiFePO₄, Solvothermal method, Surfactant.

1. INTRODUCTION

Recently, Li-ions batteries have been widely used as powder supply in electric vehicles (EVs) and energy storage. For EVs, in order to penetrate the mass market requirement, the reduction of cost and improvement electrochemical performances has become the major targets to achieve a longer driving range. This highly depends on the choice of the cathode materials, of which lithium iron phosphate (LiFePO₄) have been one of the most promising polyanion-type cathode materials. The numerous appealing features, such as excellent chemical and thermal stability, long cycling life, low

cost and environmentally friendly, make this material extensively studied all over the world since 1997 [1-3]. However, LiFePO_4 suffers from poor rate performance due to its lower charge and mass transport kinetics [4]. So far, the major obstacles of LiFePO_4 cathode with poor electronic conductivity have been overcome by applying conductive carbon coating [5-7]. Besides, metal ions doping [8-10] has been considered as an effective method to improve the sluggish lithium ion diffusion. Furthermore, fabrication of nano-size particles [11-13] have also been proposed to improve the performance of LiFePO_4 , since reduction of the grain size of cathode material may shorten the diffusion path for better Li^+ intercalation/extraction. Various LiFePO_4 nanostructures, including nanoplates [14,15], nanorods [16,17] and nanowire [18,19], have been prepared by different methods, and show significantly different electrochemical performance.

Encouraged by the self-assembly materials, many researchers have paid great attention to the organization of nanoscale building blocks into hierarchical architectures. For example, by using the self-prepared ammonium FePO_4 rectangular nanoplates as a precursor, hierarchical LiFePO_4 microflowers constructed by a number of stacked rectangular nanoplates were fabricated [20]. Such hierarchical micro/nanostructures utilize both nanometer-sized building blocks and micro-sized assemblies, resulting in better electrochemical performance. Hierarchical dumbbell-shaped LiFePO_4 mesocrystals are also prepared through solvothermal method with a mixed solvent of dimethylformamide/ethylene glycol (DMF/EG) [21]. In addition, several studies have confirmed that some organic cationic surfactants, e.g. CTAB, greatly influence the properties of the obtained powders during the hydro/solvothermal procedure [22-24]. The CTAB can not only act as dispersing agent in the specific synthesis process, but also decompose at the surface of the active material grains for better electronic conductivity. However, the amount of CTAB is a crucial parameter for the formation of the uniform hierarchical architectures.

In this work, we describe a simple solvothermal synthesis of rod-like LiFePO_4/C composite with cluster texture using PEG and water as co-solvents and CTAB as surfactant agent. The relationship of CTAB amount and the physico/electrochemical performance of LiFePO_4 is intensively studied. A possible mechanism is also proposed to understand the formation of the rod-like crystal with self-assembling architecture. The rod-like LiFePO_4/C composite with cluster texture, which is prepared with 3 mmol of CTAB, delivers a high discharge capacity of 152.3 mAh/g at 0.2C and 90.9 mAh/g at 10C.

2. EXPERIMENTAL PROCEDURE

Synthesis: Li_3PO_4 (99%, Sinopharm), $\text{FeSO}_4 \cdot 7\text{H}_2\text{O}$ (99%, Sinopharm), and H_3PO_4 (85%, Sinopharm) were used as raw materials and CTAB acted as surfactant for the preparation of LiFePO_4/C material via a solvothermal method. Firstly, the above raw materials were dissolved in 60 ml mixed solvent (30 ml polyethylene glycol (PEG) + 30 ml deionized water), forming a green precursor solution with continually stirring at room temperature. The molar ratio of Li_3PO_4 : FeSO_4 : H_3PO_4 is 1:1:0.5 and the concentration of Fe^{2+} in the final solution is 0.3 mol/L. Then, the solution was transferred into a Teflon-lined stainless steel autoclave and maintained at 180 °C for 1 h

(the heating rate was 2 °C/min). After solvothermal reaction, the grey precipitate was washed by water and ethanol several times, and then dried in a vacuum at 60 °C for 24 h. Finally, the dried powder was mixed with 20% wt of sucrose and annealed at 650 °C for 6 h under a flowing Ar (the heating rate was 5 °C/min). After cool down naturally, LiFePO₄/C cathode material was obtained. To investigate the effect of surfactant on the obtained LiFePO₄/C, different amounts of CTAB with 0, 1, 3, 5, 7, 9 mmol were introduced during the preparation of precursor solution. The corresponding samples were denoted as T1, T2, T3, T4, T5, T6, respectively.

Characterization: Crystal structures of LiFePO₄/C samples were detected by X-ray diffraction (XRD, Rigaku/DMAX-3B) using diffractometer with Cu α radiation and employed a scan rate of 0.02°/s in the 2 θ range from 10° to 70°. Particle morphology was performed on a scanning electron microscopy (SEM, FEI, Inspect F50) operated at 20 kV. Inner surface observation was detected by a high-resolution transmission electron microscopy (HRTEM, Hitachi, S4800) performed with an acceleration voltage of 200 kV.

Electrochemical measurements: the as-prepared LiFePO₄/C, carbon black and polyvinylidene fluoride (PVDF) was used as active materials, conductive additive and binder, respectively. The working electrode was prepared by mixing the above material with N-methyl pyrrolidinone (NMP, Sinopharm) in a weight ratio of 8:1:1. Then the slurry was uniformly doctor-bladed onto an aluminum current collector with a “wet” thickness of 60 μ m and further dried at 80 °C under vacuum for 12 h. The dried electrode was cut into wafer with the diameter of 13.5 mm with an overall average of 1.5 mg/cm² of electrode mass. Coin-type cells were assembled in an argon (99.999%) filled glove box with both oxygen and water contents below 0.5 ppm. Lithium metal served as counter electrode, and the electrolyte was composed of 1 mol/L LiPF₆ in ethylene carbonate and diethyl carbonate (EC/DEC, 1:1 in volume). The electrochemical tests were carried out in a battery test system (Neware, BTS3000) at various current densities between 2.0 and 4.2 V vs. Li/Li⁺ at room temperature.

3. RESULTS AND DISCUSSION

Fig.1 displays the XRD patterns of the LiFePO₄/C materials prepared with different amounts of CTAB. All the reflection peaks of the samples except T6 can be well indexed to pure phase of olivine LiFePO₄ with *Pnma* space group (JCPDS No.81-1173) without any impurity. The profiles of the diffraction lines are sharp and narrow, reflecting a good crystallinity of the samples. For T6 sample, impure phase of Li₃PO₄ is detected, demonstrating that a high level of CTAB additive may affect the purity of LiFePO₄ during solvothermal process [25]. For all samples, there is no obvious graphite peak is found in the XRD patterns. In other word, carbon may exist as amorphous phase in the lattice. It is worth to point out that the intensity of diffraction peaks increase after adding surfactant. Especially, the lattice planes of (200) and (020) change drastically by varying CTAB amounts. For instance, the peak intensity of (200) is the strongest for T3 sample with 3 mmol CTAB, while the peak intensity of (020) is the strongest for T2 sample with 1 mmol CTAB. It is well known that the cation surfactant of CTAB is easier to combine with PO₄³⁻ due to the action of coulomb force. Then the increase of the CTAB amount may promote the nucleation of LiFePO₄ because of the combination of CTAB and PO₄³⁻, resulting in some preferential orientation growth [26, 27].

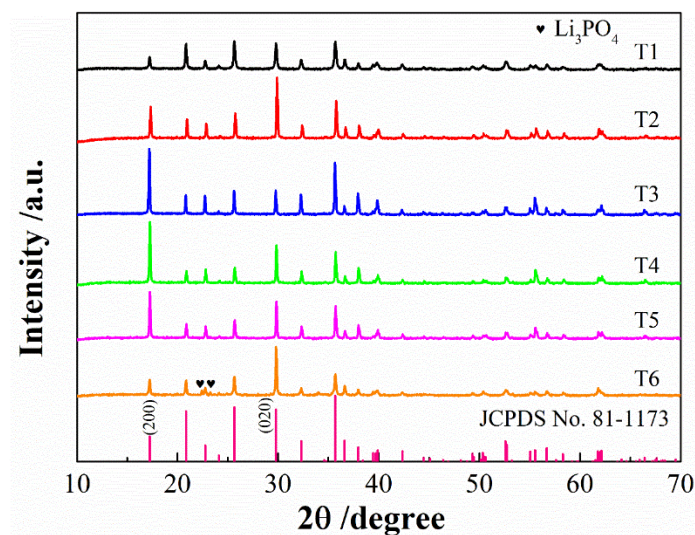


Figure 1. XRD patterns of the LiFePO_4/C materials prepared with different amounts of CTAB: T1 is 0 mmol, T2 is 1 mmol, T3 is 3 mmol, T4 is 5 mmol, T5 is 7 mmol and T6 is 9 mmol.

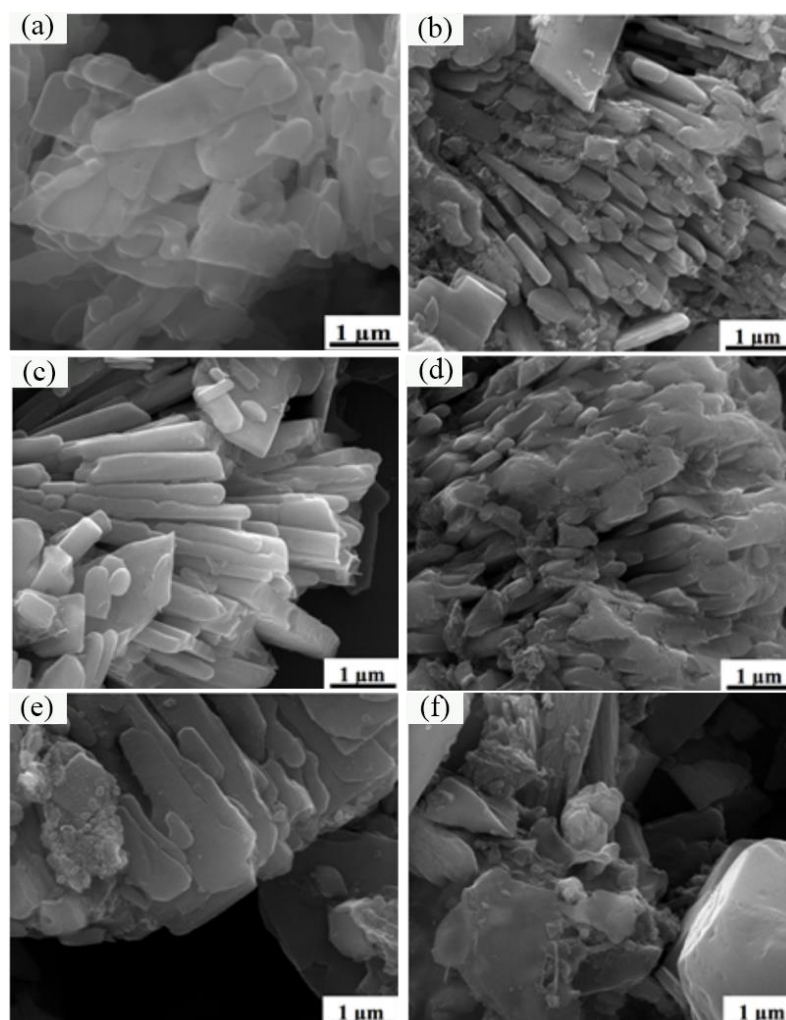
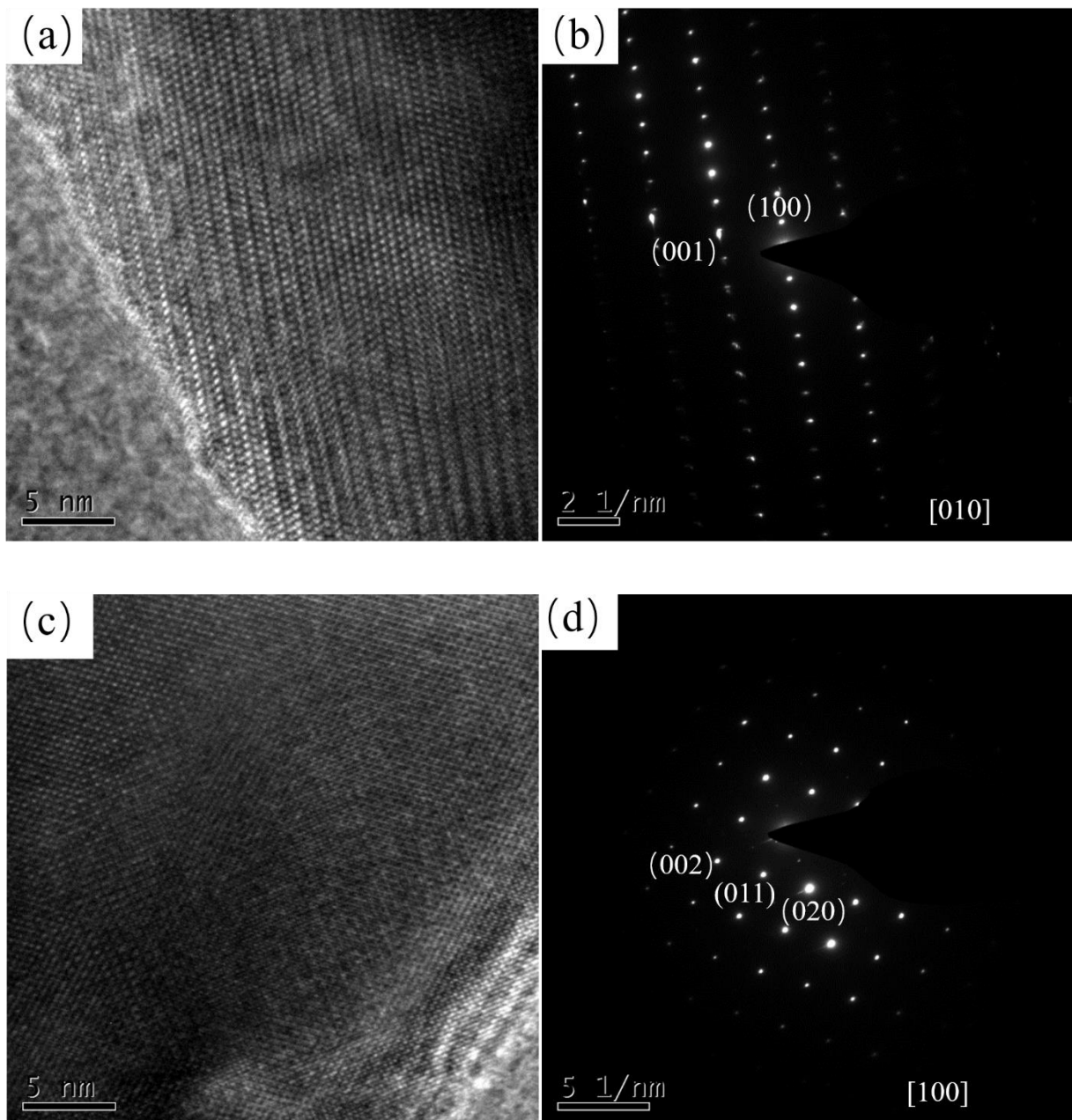


Figure 2. SEM images of the LiFePO_4/C materials prepared with different amounts of CTAB: (a) 0 mmol, (b) 1 mmol, (c) 3 mmol, (d) 5 mmol, (e) 7 mmol, (f) 9 mmol.

By comparison of the intensity ratio of reflections (020) and (200), T1 and T6 sample exhibits a much higher $I_{(020)}/I_{(200)}$ with value of 3.2 and 3.4, respectively, indicating a more pronounced orientation of the single platelets with a larger expose facet of (010) [28]. Besides, the value of $I_{(020)}/I_{(200)}$ for T3, T4 and T5 sample is 0.4, 0.7, 0.8, and 3.4, respectively, which is much lower than the standard value of LiFePO_4 ($I_{(020)}/I_{(200)}=2.1$ for JCPDS No.81-1173). As described by Ma *et al* [29], this kind of LiFePO_4 may display bc-plane (100) structure. In short, the amount of CTAB may also affect the peak intensity ratio of $I_{(020)}/I_{(200)}$, suggesting that the particles have some preferred crystal orientation.



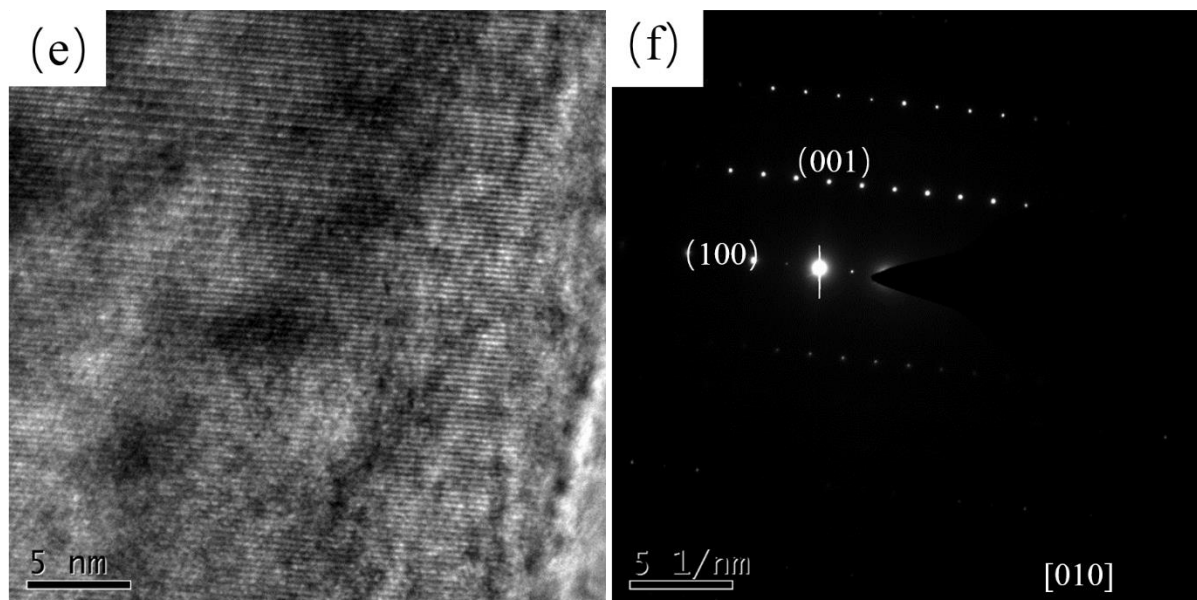


Figure 3. HR-TEM images of the LiFePO_4/C materials prepared with different amounts of CTAB: (a, b) 0 mmol, (c, d) 3 mmol, (e, f) 9 mmol.

As shown in Fig.2, SEM images of the as-prepared LiFePO_4/C were observed to investigate the effects of the added CTAB on the particle size and microstructures. From Fig.2a, the particles without CTAB show primary crystal shape of nanoplates. However, it is clearly observed that the nanoplates exhibit a random intergrowth, resulting in serious crystal agglomeration. Such plate-type structure have been widely reported in previous literature that using PEG as solvent, which indicates the formation of platelets is mainly controlled by the feature of solvent with highly viscosity and boiling point [30, 31]. After introducing CTAB surfactant, the appearance of LiFePO_4/C particle is totally different. As for T2 sample (Fig.2b), its primary particle appears as nano-rod and no intergrowth of particles is observed. On the contrary, such primary particles are closed together in an ordered direction for cluster texture, suggesting the CTAB might act as template for the self-assembly process. With the variation of the amount of CTAB, sample T3 displays good dispersion effect and well-defined morphology of rod-like particles (Fig.2c). However, T5 sample (Fig.2e) shows cluster texture composing of micro-sheet particle. This result further confirms that the CTAB surfactant play an important role in the crystal growing orientation for different microstructure. When the amount of CTAB that was added increased to 9 mmol (Fig.2f), the grains grow exceptionally with numerous fragmented nanoparticles. This can be ascribed to the decomposition of the excess CTAB into an amorphous structure during annealing process [32].

In order to further examine the inner structure of the LiFePO_4 structure, HRTEM images and the electron diffraction (ED) patterns of T1, T3 and T6 samples are recorded, as depicted in Fig. 3. In Fig.3a and b, the HRTEM and ED images reveals that the mainly exposed facet of T1 sample with nanoplates structure lays on (010), viewed along the b-direction [12]. On the contrary, Fig.3c and d illustrates that the T3 sample with rod-like primary crystal is seen to expose (100) facet [8]. Nevertheless, the plate-type particles of T6 in Fig.3 e and f is detected of revealing (010) facet. Therefore, the above result is quite agree with the XRD analysis.

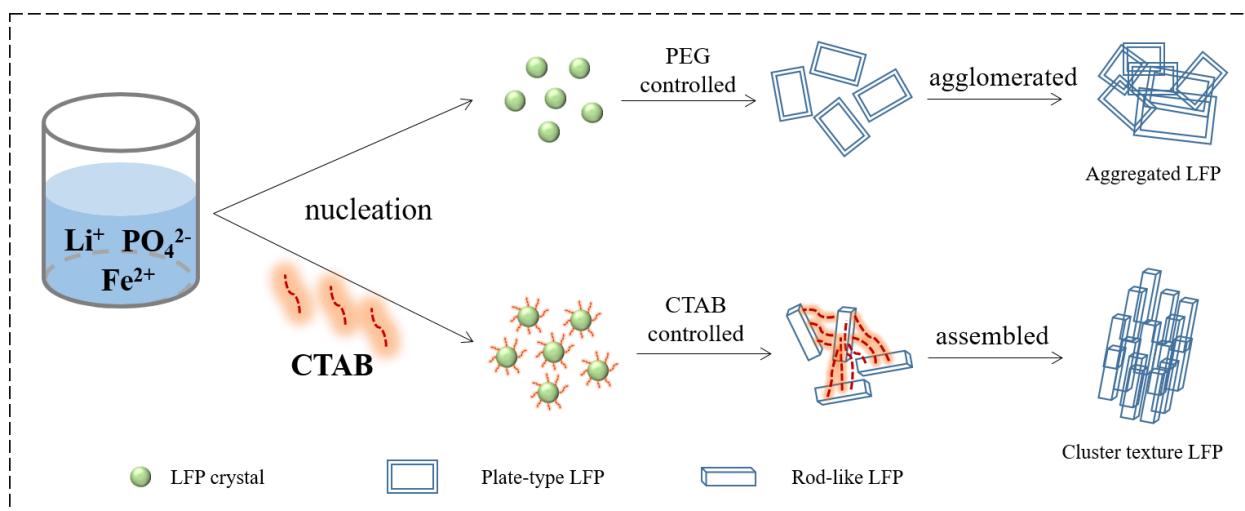


Figure 4. Schematic illustration of the formation of LiFePO_4/C particles with or without CTAB surfactant.

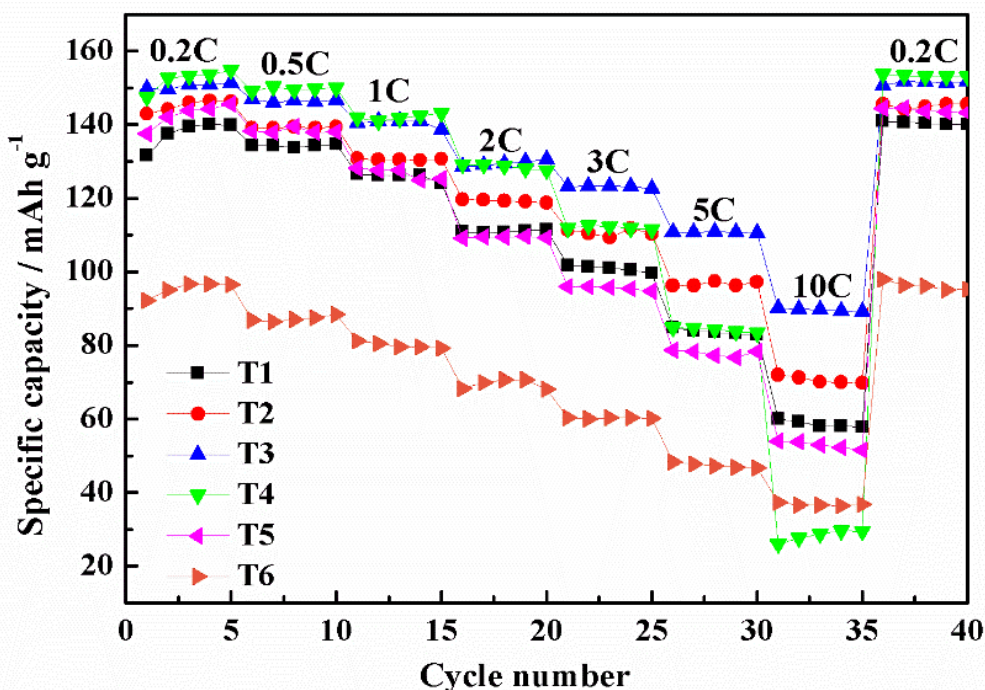


Figure 5. Rate performance of the obtained LiFePO_4/C composites with different amounts of CTAB.

Based on the above results, it can be seen that the morphologies of the LiFePO_4/C particles changes depending on the CTAB surfactant involving in the solvothermal process. As shown in Fig. 4, an anticipated mechanism for the formation of the material is proposed. In a mix solution consisted of Li^+ , PO_4^{3-} , Fe^{2+} , the formation of LiFePO_4 is based on the so called “dissolution-recrystallization process”, where the finally morphology of product is likely to form plate-type particles [33-35]. Due to the attached PEG solvent on the (010) plane by hydrogen bonds, therefore, LiFePO_4 nanoplates with larger (010) exposed surface are likely to be obtained. This can be described as a PEG controlled process. However, when CTAB is introduced into the solvent system, the nucleation and growth of LiFePO_4

nanoparticle is controlled by surfactant. On the one hand, CTAB plays a significant role in stabilizing the more reactive (100) facet of LiFePO_4 due to its preferential absorption [36]. In this condition, the morphology is mainly determined by the grow rate of [001] direction to [100] direction. Eventually, growth of (100) crystal facet have been hindered during crystallization process, resulting in rod-like primary crystal. On the other hand, the dissolve of CTAB in solvent is likely to form plenty of micelles [37]. As a result, the former rod-like particles may be connected by the CTAB micelles in an ordered arrangement in the further growth process. As the reaction proceeds, the fabrication of particles eventually lead to cluster structure where the CTAB acts as the template agent. After calcination, the residual CTAB decomposes and converts into conductive amorphous carbon on the particles surface. Nevertheless, it is obvious to seen that the amount of CTAB should be taken into consideration in the aim of homogeneous particles morphology. Too high amount of CTAB (such as 7 mmol) may lead to uneven particle shape and serious aggregation owing to the strongly hydrophobic or coulombic effects on the anions.

Fig.5 compares the rate capability of the as-prepared LiFePO_4/C particles with different amounts of CTAB, and the average discharge capacities are shown in Table S1. It is obvious to seen that in the absence of CTAB (T1 sample), the average discharge capacity is only 140.2, 137.6, 126.7, 111.4, 102.2, 85.5, 60.6 mAh/g at 0.2C, 0.5C, 1C, 2C, 3C, 5C, 10C rate, respectively. Compared to T1 sample, adding CTAB is benefit for improving the discharge capacities. In low discharge rate of 0.2C and 0.5C, the T2, T3, T4 and T5 samples show better specific capacity. In high discharge rate of 5C and 10C, T2 and T3 samples still displays excellent discharge capacity. With the amount of CTAB increases, T4 sample shows the highest capacity of 154.4 and 151 mAh/g at 0.2C and 0.5C, respectively. However, due to the irregular primary particle and serious agglomerate, this material suffers rapid capacity fading with the lowest capacity (29.4 mAh/g) at 10C. Similar with T4, as CTAB amount further increase to 9 mmol, the T6 sample shows the poor rare property, such as 96.5 and 36.7 mAh/g at 0.2C and 10C, respectively.

Table 1. Comparison of CTAB-assisted synthesized of LiFePO_4/C composites reported recently.

Solvent	Particle structure	Discharge capacities (mAh/g)				
		0.2C	1C	5C	10C	
PEG/water	Cluster texture	152.3	142.2	110.1	90.9	This work
Alcohol/water	Leaf-like and spherical	110	101	95	90	[22]
Water	Porous structure	152.1 (0.1C)	115	---	---	[38]
DMF/EG	Plate-architecture	145.7(0.1C)	130.7	---	---	[39]
EG	Hollow micro-spheres	163 (0.1C)	145	137	118	[40]
Water	Hollow spheres	135 (0.1C)	125	112	103	[41]

Among all the samples, when adding 3 mmol CTAB surfactant, the obtained LiFePO_4/C delivers the best rate performance and capacities as high as 152.3, 148.6, 142.2, 130.5, 124.8, 110.1 and 90.9 mAh/g at 0.2, 0.5, 1, 2, 3, 5, 10C rate, respectively. Such result is better than that of porous LiFePO_4/C synthesized via hydrothermal route in our previous work [38], and the electrochemical performances presented in this work are compared with other CTAB-assisted synthesis of LiFePO_4/C

composites reported in the literatures [22, 39-41], which is displayed in Table 1. The most likely reason can be attributed to the shorter ion diffusion path of (100) facet and the ordered crystal arrangement of cluster architecture provide flexible texture for charge/discharge process.

4. CONCLUSION

A surfactant assisted solvothermal synthesis method is employed to prepare LiFePO₄/C composite with using PEG/H₂O as co-solvent and CTAB as surfactant. Results show that the amount of CTAT greatly influences the orientation crystal growth and particle morphology, which leads to significant changes in the electrochemical behavior of the LiFePO₄/C cathode material. The reason may be account for the attachment of CTAB on the crystal facet, as long as its template function during synthesis procedure. Among all the sample, the best rate performance is obtained by using a specific amount (3 mmol) of CTAB. The as-prepared LiFePO₄/C shows rod-like primary particles with (100) exposed facet and the self-assembly cluster texture, exhibiting a high discharge capacity of 152.3 and 90.9 mAh/g at 0.2C and 10C, respectively. Such feature of cluster architecture is favorable to shorter electron and ion diffusion path for high rate electrochemical performance, which may expand the application field of lithium-ion batteries.

ACKNOWLEDGMENTS

This work was supported by the National Natural Science Foundation of China (No. 51364021), the project of Natural Science Foundation of Yunnan Province (No. 2014FA025), the project of Academician's Discovering Found from Yunnan Provincial Science and Technology Department (No. 2015HA016, No. 2016HA011), the Program for Innovative Research Team in University of Ministry of Education of China (No. IRT_17R48), and the author appreciate the TEM tested by Analysis and Testing Foundation of Kunming University of Science and Technology.

References

1. A.K. Padhi, K.S. Nanjundaswamy and J.B. Goodenough, *J. Electrochem. Soc.* 177 (1997) 1188.
2. J.B. Goodenough and K.S. Park, *J. Am. Chem. Soc.*, 135 (4) (2013) 1167.
3. J.M. Tarascon and M. Armand, *Nature*, 414 (2001) 359.
4. K.M.Ø, Jensen, M. Christensen, H.P. Gunnlaugsson, N. Lock, E.D. Bøjesen, T. Proffen and B.B. Iversen, *Chem. Mater.*, 25 (2013) 2282.
5. Y. Yao, P. Qu, X. Gan, X. Huang, Q. Zhao and F. Liang, *Ceram. Int.*, 42 (2016) 18303.
6. X. Huang, Y. Du, P. Qu, F. Liang, Y. Dai, Y. Yao, *Int. J. Electrochem. Sci.*, 12 (2017) 7183.
7. D. Zhou, X. Qiu, F. Liang, S.C. Cao, Y. Yao, X. Huang, W. Ma, B. Yang and Y.N. Dai, *Ceram. Int.*, 43 (2017) 13254.
8. H. Yuan, X. Wang, Q. Wu, H. Shu and X. Yang, *J. Alloys Compd.*, 675 (2016) 187.
9. X. Huang, F. Liang, Y. Du, K. Zhang, Y. Yao and Y. Dai, *Nano*, 11 (2016) 1650122-1.
10. H.C. Liu, Y.M. Wang and C.C. Hsieh, *Ceram. Int.*, 43 (2017) 2378.
11. J. Liu, Z. Wang, G. Zhang, Y. Liu and A. Yu, *Int J. Electrochem. Sci.*, 8 (2013) 2842..
12. L. Wang, W. Sun, X. Tang, X. Huang, X. He, J. Li, Q. Zhang, J. Gao, G. Tian and S. Fan, *J. Power Sources*, 244 (2013) 94.
13. Y. Liu, J. Gu, J. Zhang, J. Wang, N. Nie, Y. Fu and W. Li, *Electrochim. Acta*, 173 (2015) 448.

14. R. Mei, X. Song, Y. Yang, Z. An and J. Zhang, *RSC Adv.*, 4 (2014) 5746.
15. C. Nan, J. Lu, C. Chen, Q. Peng and Y. Li, *J. Mater. Chem.*, 21 (2011) 9994.
16. L. Bao, G. Xu, X. Sun, H. Zeng, R. Zhao, X. Yang, G. Shen, G. Han and S. Zhou, *J. Alloys Compd.*, 708 (2017) 685.
17. Y. Wang, B. Zhu, Y. Wang and F. Wang, *Ceram. Int.*, 42 (2016) 10297.
18. L. Peng, Y. Zhao, Y. Ding and G. Yu, *Chem. Commun.*, 50 (2014) 9569
19. S. Lim, C. S. Yoon and J. Cho, *Chem. Mater.*, 20 (2008) 4560.
20. Q. Wang, W. Zhang, Z. Yang, S. Weng and Z. Jin, *J. Power Sources*, 196 (2011) 10176.
21. N. Zhou N, H.Y. Wang, E. Uchaker, M. Zhang, S.Q. Liu and Y.N. Liu, *J. Power Sources*, 239 (2013) 103.
22. F. Di Lupo, G. Meligrana, C. Gerbaldi, S. Bodoardo and N. Penazzi, *Electrochim. Acta*, 156 (2015) 188.
23. Y. Yu, Q. Li, Y Ma, X. Zhang, Y. Zhu and Y. Qian, *J. Nanosci. Nanotechno.*, 13 (2) (2013) 1515.
24. M.H. Lee, J.Y Kim and H.K. Song, *Chem. Commun.*, 46 (36) (2010) 6795.
25. D. Choi and P.N. Kumta, *J. Power Sources*, 163(2) (2007) 1064.
26. K. Dokko, S. Koizumi, H. Nakano and K. Kanamura, *J. Mater. Chem.*, 17 (2007) 4803.
27. H. Yan, X. Zhang, J. Wu, L. Wei, X. Liu and B. Xu, *Powder Technol.*, 188 (2008) 128.
28. L. Wang, X. He, W. Sun, J. Wang, Y. Li and S. Fan, *Nano Lett.*, 12 (2012) 5632.
29. Z. Ma, G. Shao, Y. Fan, G. Wang and J. Song, *ACS Appl. Mater. Inter.*, 6 (2014) 9236.
30. C. Gong, F. Deng, C. Tsui, Z. Xue, Y.S. Ye, C.Y. Tang, X. Zhou and X. Xie, *J. Mater. Chem. A*, 2 (2014) 19315.
31. S. Yang, X. Zhou, J. Zhang and Z. Liu, *J. Mater. Chem.*, 20 (2010) 8086.
32. H. Wang, M. Yang, Y. Gong, L. Feng, C. Dang, Y. Shi, Q. Shi, J. Wei, Z. Liao and T. Lu, *Ceram. Int.*, 43 (2017) 5680.
33. D. Choi, D. Wang, IT. Bae, J. Xiao, Z. Nie, W. Wang, V.V. Viswanathan, Y.J. Lee, J.G. Zhang, G.L. Graff, Z. Yang and J. Liu, *Nano Lett.*, 10. (2010) 2799.
34. C. Xu, L. Wang, X. He, J. Luo, Y. Shang and J. Wang, *Int. J. Electrochem. Sci.*, 11 (2016) 1558.
35. D. Carriazo, M.D. Rossell, G. Zeng, I. Bilecka, R. Erni and M. Niederberger, *Small*, 8 (2012) 2231.
36. R. Liu, Z. Ji, J. Wang and J. Zhang, *Appl. Surf. Sci.*, 441 (2018) 29.
37. B. Pei, Z. Jiang, W. Zhang, Z. Yang and A. Manthiram, *J. Power Source*, 239 (2013) 475.
38. F. Liang, Y. Yao, Y. Dai, B. Yang, W. Ma and T. Wantanabe, *Solid State Ionics*, 214 (2012) 31.
39. S.C. Zhang, G.R. Liu, X. Wei and X. X. Lu, *Proceedings of International Conference*, 2 (2013) 02PCN28.
40. Y. Liu, J. Zhang, Y. Li, Y. Hu, W. Li, M. Zhu, P. Hu, S. Chou and G. Wang, *Nanomaterials*, 7 (2017) 368.
41. M.H. Lee, T.H. Kim, Y.S. Kim and H. -K. Song, *J. Phys. Chem. C.*, 115 (2011) 12255.